New Materials, Compounds and Applications
Vol.7, No.1, 2023, pp.5-14

ADVANTAGE OF PET ON POLYMERS IN MAGNETIZATION IN COMPOSITE MATERIAL WITH NANOMETRIC OXIDES

Pedro Vera-Serna[1*], Felipe Nerhi Tenorio-González[1], Aristeo Garrido-Hernández[2], Tania López Castro[1], Graciela M. Cetina-Quijano[1]

[1] Universidad Politécnica de Tecámac, División de Ingenierías, Tecámac, México, México
[2] Universidad Tecnológica de Tecámac, Tecámac, México, México

Abstract. This study deals with the magnetic properties of the MnO_2-Fe_2O_3-polymer composite, the polymers employed were Low-Density Polyethylene (LDPE), Polycarbonate (PC), Polylactic acid (PLA) and Polyethylene terephthalate (PET). Iron oxide and manganese oxide particles were reduced to a nanometric scale using a high-energy Mixer/Miller before being used in the composite elaboration. The composites were prepared using a specific MnO_2:Fe_2O_3:polymer ratio. X-Ray patterns revealed that the MnO_2 Fe_2O_3 powders crystallized in the same phases with deformations. Scanning Electron Microscopy showed that the MnO_2 and Fe_2O_3 morphology of the powders was irregular. MnO_2-Fe_2O_3-PET exhibited a magnetization higher than the other polymers and an electrical resistance of 200 GigaOhms. Finally, the heat treatment temperature required to create the composites was much lower than the melting point of ceramics method.

Keywords: *PET, PLA, LDPE, Magnetization, Composites, Iron oxide.*

Corresponding Author: *Pedro Vera Serna, Universidad Politécnica de Tecámac, División de Ingenierías, 55740, Tecámac, México, México*, *e-mail: pedrovera.upt@gmail.com*

Received: *15 January 2023;* ***Accepted:*** *24 March 2023;* ***Published:*** *17 April 2023.*

1. Introduction

Magnetization has been studied for several decades in various materials (Cerdan *et al.,* 2022), including metallic, polymer, ceramic, and composite materials (Babashov *et al*., 2021). These materials have been developed for various applications such as memory devices, medical valves, ferrofluid materials, pigments, communication elements, hyperthermia treatments, magnetic sensors, storage data, nanodevices, and others (Cgesnitskiy *et al.*, 2022). However, with the advancements in technology, there has been an increased focus on improving products, materials, and services. As a result, the approach for application development has changed, and there is now a need to create cheap, renewable materials that can be processed with low energy (Bang *et al.*, 2019) while still being easy to manipulate and having better properties than existing commercial products (Hu *et al.*, 2020).

In 2020, a study on the magnetization of Fe_3O_4-polymer composites demonstrated a soft ferromagnetic behavior. Previous work in 2012 reported that Fe_3O_4 nanoparticles had a magnetization of 38 emu/g; the particle presented nanometric size and was

How to cite (APA):
Vera-Serna, P., Tenorio-González, F.N., Garrido-Hernández, A., López Castro, T., & Cetina-Quijano, G.M. (2023). Advantage of pet on polymers in magnetization in composite material with nanometric oxides. *New Materials, Compounds and Applications*, *7*(1), 5-14.

synthesized using the hydrothermal method. The magnetization values were similar to those of polyamide 6 (Zhang & Zhu, 2012). Over the past 20 years, various polymer materials have been developed to respond to various stimuli. For instance, Lingjuan reported on the synthesis and properties of magnetic particles and polymers, discussing particle size, the distance between particles, and the magnetic properties of embedded particles in the polymer (Lingjuan *et al.*, 2022). In the same year, an interesting extrusion process was developed by Christian Huber et al. to study the properties of polymer-bonded anisotropic $SrFe_{12}O_{19}$. The researchers used filaments for fused filament fabrication using a 3D printer, demonstrating a line of research to develop composite materials using polymers and magnetic materials for novel applications (Huber *et al.*, 2020).

The advanced ceramics materials under traditional method need high energy to get crystal structures as spinel, and in various cases the materials with spinel structure obtained by mechanosynthesis need annealing treatment to have the form using a mold to get the shape required (Salazar-Tamayo *et al.*, 2019), sometimes the treatment thermic reduce the value of magnetic saturation, on this line were studied different polymers to try to maintain the value of magnetization in temperatures under 270 °C.

Traditional methods for producing advanced ceramic materials typically require significant energy input to achieve crystal structures such as spinel. In many cases, materials with a spinel structure produced via mechanosynthesis require annealing treatment and use of molds to obtain a desired shape (Salazar-Tamayo *et al.*, 2019). However, heat treatment can decrease magnetic saturation value, it is a problem. To mitigate this issue, various polymers have been investigated for their potential to form composite materials while maintaining magnetic saturation values. Typically, the heat treatments involved in producing these composites are kept below 270°C in this study. Literature has demonstrated that the magnetic saturation of iron and manganese oxides decrease when the temperature increase (Caizer, 2016). In this vein, it is possible using polymers and preparing composites to avoid magnetization variations in MnO_2 and Fe_2O_3 obtained by milling.

Soft magnetic ceramic materials with temporal magnetization have applications in transformer cores, while hard magnetic materials that have permanent magnetization is used in electric generators. The crystal structure defectively affects magnetization (De Julian Fernandez, 2021) since it depends on the atoms position of the elements in the material. X-Ray Diffraction is a fundamental technique to elucidate the atoms position because it can be used for identifying the material phases (Salazar-Tamayo *et al.*, 2019).

In this research, the particle size of magnetic MnO_2-Fe_2O_3 powders was reduced using a high-energy miller. These powders were embedded in Low-Density Polyethylene (LDPE), Polycarbonate (PC), Polylactic acid (PLA), and Polyethylene terephthalate (PET) polymers. The characterization focused on magnetization values, electric resistance, and homogeneity of the composite materials.

2. Experimental

To achieve composites that exhibit a magnetic response, four polymers were employed. The desired shape for a specific application was attained through a heat treatment process that permitted the combination of ceramic powders and polymers within a recipient.

For a better presentation of the results, the composites were named as follows:

Table 1. Composites

Composites	Oxides		Polymer
COMP A	MnO_2	Fe_2O_3	LDPE
COMP B	MnO_2	Fe_2O_3	PC
COMP C	MnO_2	Fe_2O_3	PLA
COMP D	MnO_2	Fe_2O_3	PET

Before preparing the polymer composite, the following steps were executed.

1. Powders milling
2. Characterization of powders (MnO_2-Fe_2O_3) after 12 hours of milling (Structural, morphology, particle size, and magnetic response)
3. Composites elaboration (COMP A. COMP B, COMP C, and COMP D)
4. Composites characterization.

2.1. Powders milling

The MnO_2 and Fe_2O_3 powders (Sigma-Aldrich, >99%) were milled for 12 hours in a mixer/mill SPEX 8000D. Throughout the milling process, 4 steel balls, each with a diameter of 12.7 mm, were utilized in 60 cm^3 vials. The ball-powder mass ratio for the reduction of oxide powder was 20:1.

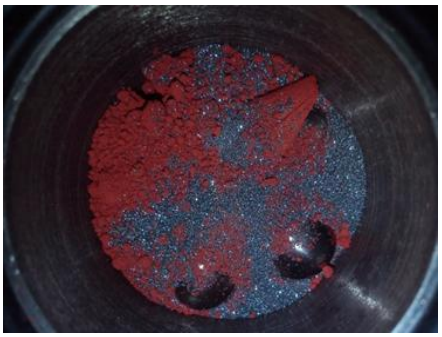

Fig. 1. Oxides in vial with iron balls

2.2. Characterization of powders

Characterization is crucial to determine the crystal structure, morphology, particle size, and magnetization of oxide powders after 12 hours of milling. The structural characterization was performed by X-Ray Diffraction (XRD) using a Philips PW1710 instrument with Co radiation (Kα=0.17902 nm). Material Analysis Using Diffraction (MAUD) software was employed for identifying the crystalline phases. The morphology of the powders was observed through a Jeol Scanning Electron Microscope (SEM) model Jsmh 6010 at 20kV, while particle size was evaluated using a Brookhaven Nanoplus 90 analyzer. The level of magnetization was assessed using a MicroSense EV7 magnetometer (VSM-EV7) at 18,000 Oersteds.

2.3. Develop of composites

The composites were produced within a Mondragon furnace model HR-12-2/1200-ER. The temperature was set above the melting temperature of each polymer employed. The polymer was added in pellet form, and the powders were added on top of the pellets. As the temperature increased, the pellets became liquid, and the materials were mixed to obtain a homogeneous composite. Afterward, the composite was cooled to room temperature.

2.4. Characterization of composites

The composites were obtained at a relatively low temperature, the process does not affect the crystal structure of MnO_2 and Fe_2O_3 requires higher temperatures to be modified. As the composite was a continuous shape, the particle size evaluation was not reported. Therefore, only the embedded ceramic powders into the polymer were observed. The image of the composite was obtained through an Optic Microscope Mitutoyo 176-812A with a Len PF 10X/18 mm. The magnetic evaluation was conducted using a MicroSense EV7 magnetometer (VSM-EV7) at 18,000 Oersteds. The electric resistance was measuring with a megohmmeter AMPROBE AMB-5KV and finally was observed in SEM.

3. Results and discussion

3.1. Powder milling

Fig. 2 displays the powders obtained by milling, which have a dark color and an irregular morphology, as determined by the scanning electron microscope (Fig. 3). The deformation, fractures, and welded particles during the milling process lead forming of irregular morphology. This observation is consistent with previous reports on this process, and the color of the powders is similar to that of ferrites obtained through mechanochemical methods (Ban, 2019).

Fig. 2. MnO_2-Fe_2O_3 powders after 12 h milling

3.2. Characterization of powders

Fig. 3 illustrates the crystalline structures of MnO_2 and Fe_2O_3 powders. The Rietveld analysis, conducted using the MAUD software, revealed that after 12 hours of milling, the powders had crystallized the same phases, which were identified by their respective phase. The peak width was influenced by the deformation of the powders during the milling process, as Gouvea reported. The XRD patterns of the 12-hour milled powders did not indicate the presence of any secondary phases (Gouvea, 2022). The SEM morphology (shown in Fig. 4) demonstrated that the powders had irregular shapes, consistent with the findings reported by other researchers (Ksepko & Lysowski, 2021).

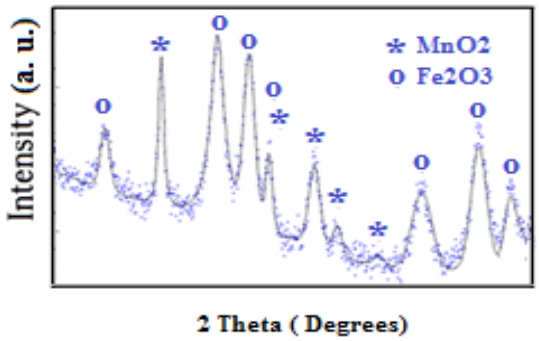

Fig. 3. The profile of XRD using Rietveld method on 12 hours of milling

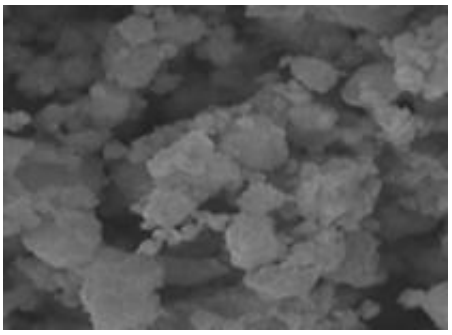

Fig. 4. Irregular morphology in powders under 12 hours

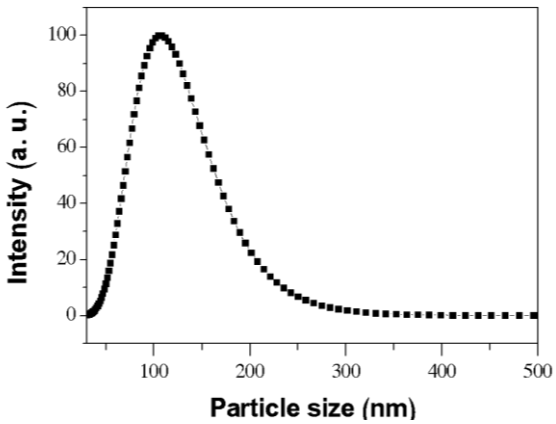

Fig. 5. Particle size distribution of MnO_2 and Fe_2O_3 powders after 12 h of milling

After 12 hours of milling, the particle size distribution analysis of the MnO_2 and Fe_2O_3 powders revealed the presence of nanometric particles (50-250 nm, as shown in Fig. 5). This finding is promising for producing composite materials since smaller particle size ensures a homogeneous distribution within the composite, in contrast to larger particles, only the size of particle was observed with the milling, the crystal structure was the same.

3.4. Composite characterization

To get the composites, the powders obtained on 12 hours of milling were added to metal recipient on pellets of every polymer, the results were the composites COMP A, COMP B, COMP C and COMP D.

A beam of light was passed through each polymer composite to identify the homogeneity of the polymer composites and determine the powder's distribution within the material. The distribution of the powders was also observed using an optical microscope Fig. 6.

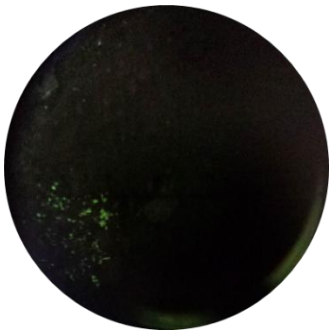

Fig. 6. Composite COMP A under optic microscope

In Fig. 6, the distribution of the powder in polymer composite was observed to be nearly impermeable to light when LDPE polymer was used in the composite. This indicates that a more effective process is needed to achieve complete homogeneity. In contrast, in COPM B, a larger amount of light was able to pass through the material, demonstrating the ability of the material to allow a greater quantity of light to permeate the composite (see Fig. 7).

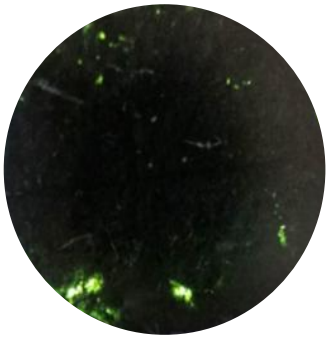

Fig. 7. Composite COMP B under optic microscope

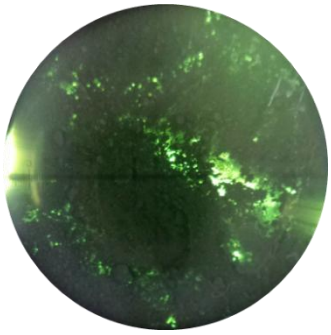

Fig. 8. Composite COMP C under optic microscope

Based on the results shown in Fig. 9, the polymer composite with the best powder distribution was COMP D, which used PET as the continuous matrix. This composite was found to be impermeable to the beam of light, indicating that the particles were well-distributed within the material.

Fig. 9. Composite COMP D under optic microscope

The polymer composites (COMP A, COMP B, COMP C, and COMP D) were evaluated using an optical microscope to observe their appearance under light (Fig. 10). Among these composites, COMP D displayed the most homogeneous distribution, which can be influenced by the melting point of the PET.

Magnetization

The magnetization results of the polymer composites were obtained using a magnetometer; the polymer composite with the highest magnetization 0.6 emu/g was COMP D (Fig. 11). This finding is consistent with the literature, which reports a 0.5 emu/g magnetization (Fatemeh *et al.*, 2019). The high magnetization values observed in COMP D might be attributed to the absence of magnetic domains in PET, well-distributed nanoparticles, thin cover on particles and better sealed on surface of particles agglomerates.

Electric resistance

The electrical resistance of composite COMP D was evaluated to be 200 GigaOhms (shown in Fig. 12). This high electrical resistance is beneficial in reducing losses due to heating, as materials with lower electrical resistance tend to experience greater electric losses when heated (Leuning *et al.*, 2021). Furthermore, previous studies

on magnetic and electrical materials have demonstrated that adding Mn can increase electrical resistance and reduce core losses at specific high frequencies (Elgamli *et al.*, 2023).

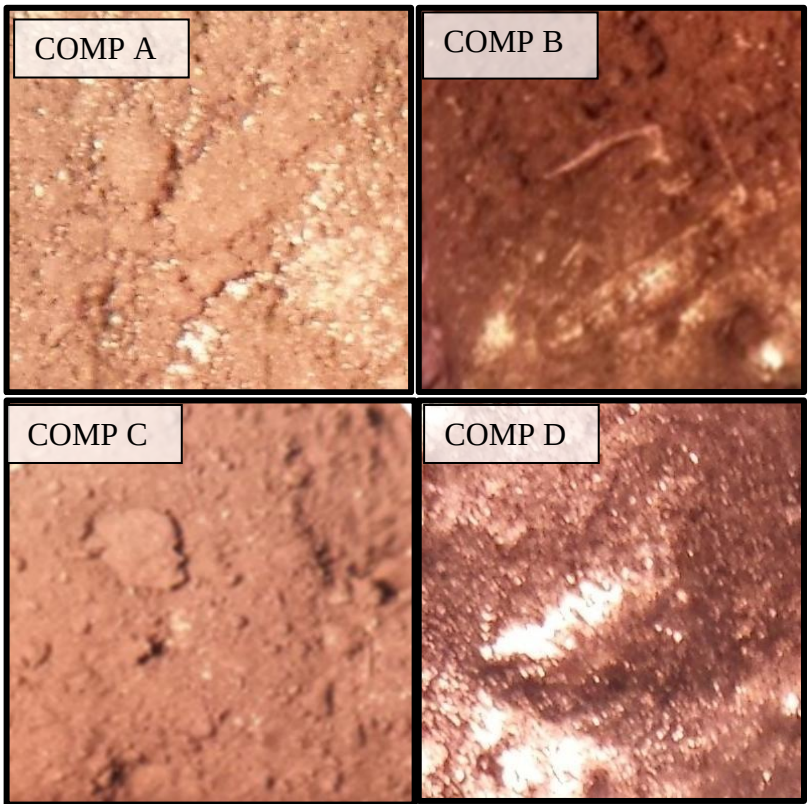

Fig. 10. Optical image of COMP A, COMP B, COMP C and COMP D

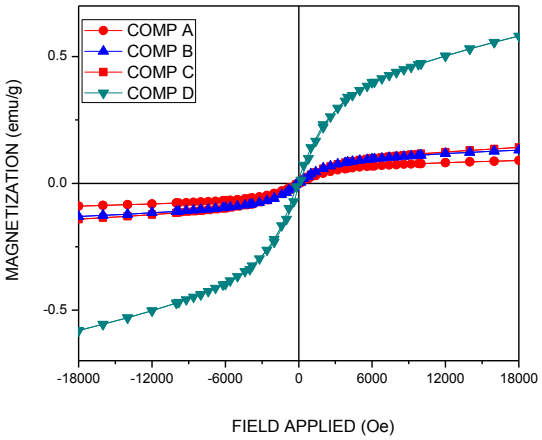

Fig. 11. Magnetization of polymer composites

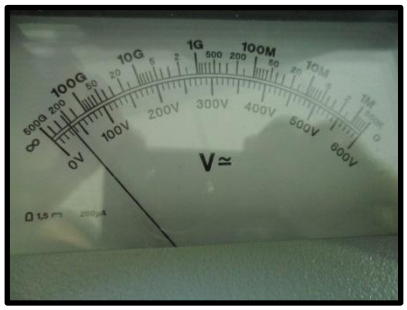

Fig. 12. Electric resistance of composite COMP D

SEM imaging of COMP D revealed an appropriate distribution of the MnO2 and Fe2O3 powders in PET, despite the fact that the powders are not soluble in PET. This finding is consistent with previous studies (Xu *et al.*, 2020), where it was observed that PET can effectively cover the powders as a film. Due to its viscosity, PET is able to achieve good distribution of powders, as shown in Fig.13.

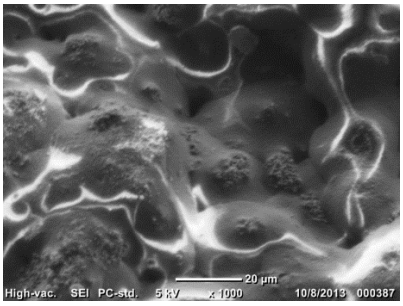

Fig. 13. Image of Composite COMP D

4. Conclusion

The MnO_2-Fe_2O_3-PET composite exhibited superior properties in terms of magnetization and homogeneity, which make it suitable for a variety of product applications with different shapes. The high electric resistance of the composite indicates low loops in the material on electric currents, making it a desirable property. After 12 hours of milling, the powders achieved a nanometric particle size. MnO_2-Fe_2O_3 powders embedded in PLA, LDPE, and PC showed lower values on magnetic saturation, fissures, and an inferior powder distribution than its counterpart COMP D.

References

Babashov, V.G., Suleimanov, S.K., Daskovskii, M.I., Shein, E.A. & Stolyankov, Y.V. (2021). Structure and properties of highly porous alumina-based ceramic materials after heating by concentrated solar radiation. *The Journal of Ceramic*, *5*(1), 24-33 https://doi.org/10.3390/ceramics5010003

Bang, S., Pin, Z., Sijin, C., Haiping, Y., Nanwen, Z., Tonghua, S. & Ziyang L. (2019). Manganese-based catalysts recovered from spent ternary lithium-ion batteries and its catalytic activity enhanced by a mechanical method, *Journal of Cleaner Production, 213* (2019), 1346-1352 https://doi.org/10.1016/j.jclepro.2018.12.248

Caizer, C. (2016). Nanoparticle size effect on some magnetic properties. *Handbook of Nanoparticles*, 475–519. doi:10.1007/978-3-319-15338-4_24

Cerdan, K., Moya, C., Van Puyvelde, P., Bruylants, G. & Brancart J. (2022). Magnetic Self-Healing Composites: Synthesis and Applications, *Molecules*, *27*(12), 3796 http://dx.doi.org/10.3390/molecules27123796

Cgesnitskiy, A.V., Gayduk, A.E., Seleznev, V.A., & Prinz, V.Y. (2022). Bio – inspired micro – and nanorobotics driven by magnetic field, *15*(21), 7781, https://doi.org/10.3390/ma15217781.

De Julian Fernandez, C., Sangregorio, C., De La Figuera, J., Belec, B., Makovec, D., & Quesada, A. (2021). Progress and prospects of hard hexaferrites for permanent magnet applications. *Journal of Physics D: Applied Physics*, *54*(15), 153001. doi:10.1088/1361-6463/abd272.

Elgamli, E., Anayi, F. & Shouran, M. (2023). Impact of manganese diffusion into non-oriented electrical steel on power loss and permeability at different temperatures. *Front. Mater.*, 9, 1108308. doi: 10.3389/fmats.2022.1108308.

Fatemeh, M., Majid, M., & Masoud, L. (2019). Microwave absorption and photocatalytic properties of magnetic nickel nanoparticles/recycled PET nanofibers web, *The Journal of The Textile Institute*, *110*(11), 1606-1614, doi:10.1080/00405000.2019.1612501.

Gouvea, E.d.S., Rossi, M.C., Escuder, A.V., Afonso, C.R.M., & Borrás, V.A., (2022). Relation between Mechanical Milling Parameters in Phase Transformation and Oxygen Content in Ti–Nb–Mo Powders for Posterior Sintering. *Metals*, 12, 1238, https://doi.org/10.3390/met12081238.

Hu, L., Wang, Q., Zhang, X., Zhao, H., Cui, Z., Fu, P., ... & Qiao, X. (2020). Light and magnetism dual-gated photoinduced electron transfer-reversible addition–fragmentation chain transfer (PET-RAFT) polymerization. *RSC Advances*, *10*(12), 6850-6857.

Huber, C., Cano, S., Teliban, I., Schuschingg, S., Groenefeld, M., & Suees, D. (2020). Polymer – bonded anisotropic $SrFe_{12}O_{19}$ filaments for fused filament fabrication. *Journal of Applied Physics*, *127(*6), 063904, doi:10.1063/1.5139493.

Ksepko, E., Lysowski, R. (2021). Reactivity study of bimetallic Fe-Mn oxides with addition of TiO2 for chemical looping combustion purposes. *Catalysts*, *11*(12), 1437 http://dx.doi.org/10.3390/catal11121437

Leuning, N., Jaeger, M., Schauerte, B., Stöcker, A., Kawalla, R., Wei, X., ... & Hameyer, K. (2021). Material design for low-loss non-oriented electrical steel for energy efficient drives. *Materials*, *14*(21), 6588. http://dx.doi.org/10.3390/ma14216588

Li, R., Zhang, M., Fu, X., Gao, J-, Huang, C-, Li, Y. (2022), Research of low – dimensional carbon – based magnetic materials, *ACS Appl. Electron. Mater*, *4*(7), 3263-3277, https://doi.org/10.1021/acsaelm.2c00407

Sinha, A., Bortolotti, M., Ischia, G., Lutterotti, L., & Gialanella, S. (2022). Electron diffraction characterization of nanocrystalline materials using a Rietveld-based approach. Part I. Methodology. *Journal of Applied Crystallography*, *55*(4), 953–965, https://doi.org/10.1107/S1600576722006367.

Salazar-Tamayo, H., Tellez, K.E.G. & Meneses, C.A.B. (2019).Cation Vacancies in NiFe2O4 During Heat Treatments at High Temperatures: Structural, Morphological and Magnetic Characterization. *Mat. Res.*, *22(*5), 1-11. https://doi.org/10.1590/1980-5373-MR-2019-0298

Xu, A., Wang, Y., Xu, X., Xiao, Z., & Liu, R. (2020). A Clean and Sustainable Cellulose-Based Composite Film Reinforced with Waste Plastic Polyethylene Terephthalate. *Advances in Materials Science and Engineering, 2020* (7323521), 1-7, https://doi.org/10.1155/2020/7323521.

Zhang, H., Zhu, G. (2012). One-step hydrothermal synthesis of magnetic Fe3O4 nanoparticles immobilized on polyamide fabric. *Applied Surface Science*, *258*(11), 4952-4959.